Published in final edited form as:
Neuron. 2012 December 6; 76(5): 931–944. doi:10.1016/j.neuron.2012.10.009.

Dystroglycan organizes axon guidance cue localization and axonal pathfinding

Kevin M. Wright[1], **Krissy Lyon**[1], **Haiwen Leung**[3], **Daniel J. Leahy**[2], **Le Ma**[3], and **David D. Ginty**[1,4]

[1]The Solomon H. Snyder Department of Neuroscience and Howard Hughes Medical Institute, The Johns Hopkins University School of Medicine, Baltimore, MD 21205

[2]The Department of Biophysics and Biophysical Chemistry, The Johns Hopkins University School of Medicine, Baltimore, MD 21205

[3]Zilkha Neurogenetic Institute, Department of Cell and Neurobiology, Keck School of Medicine, University of Southern California, 1501 San Pablo Street, Los Angeles, CA 90089, USA

Abstract

Precise patterning of axon guidance cue distribution is critical for nervous system development. Using a murine forward genetic screen for novel determinants of axon guidance, we identified B3gnt1 and ISPD as required for the glycosylation of dystroglycan *in vivo*. Analysis of *B3gnt1, ISPD* and *dystroglycan* mutant mice revealed a critical role for glycosylated dystroglycan in the development of several longitudinal axon tracts. Remarkably, the axonal guidance defects observed in *B3gnt1, ISPD* and *dystroglycan* mutants resemble those found in mice lacking the axon guidance cue Slit and its receptor Robo. This similarity is explained by our observations that dystroglycan binds directly to Slit and is required for proper Slit localization within the basement membrane and floor plate *in vivo*. These findings establish a novel role for glycosylated dystroglycan as a key determinant of axon guidance cue distribution and function in the mammalian nervous system.

Introduction

Precise temporal and spatial expression patterns of extrinsic instructive cues in the embryonic nervous system establish the fidelity of developmental processes, including morphogenesis, neuronal differentiation, polarization, axon guidance, and synaptogenesis. Axon guidance is particularly reliant on proper cue presentation because axons must often navigate long distances in discrete sequential steps, with intermediate targets providing precisely positioned instructional cues that orient axons towards their next guidepost *en route* to final target fields (Garel and Rubenstein, 2004). Recently, axon guidance defects have been implicated in several human neurological disorders, although the molecular etiology underlying these defects is poorly understood (Engle, 2010).

Axon guidance cues can function as attractants or repellants by binding to cell surface receptors that transduce guidance information through signaling cascades that reorganize the

[4]Corresponding author: dginty@jhmi.edu, ph. 410-614-9494.

actin cytoskeleton within growth cones (Vitriol and Zheng, 2012). These cues, which include members of the Slit, Netrin, Semaphorin, and Ephrin families of ligands, are expressed in or around intermediate and final target fields, or on neurons themselves, whereas their respective receptors are expressed on axonal growth cones (Kolodkin and Tessier-Lavigne, 2011). Several axon guidance cues, such as Class 4–7 Semaphorins and Ephrins, are either transmembrane or tethered to the plasma membrane of the expressing cell through a GPI-linkage and therefore function primarily as short-range cues. In contrast, Slits, Netrins, Neurotrophins, and Class 3 Semaphorins, as well as morphogens of the Wnt, Hedgehog, and TGFβ families, are secreted cues and may regulate axonal growth and guidance at both long and short range.

Extending axons encounter multiple attractive or repulsive guidance cues, sometimes simultaneously, along their trajectory. The complexity of integrating signals from multiple guidance cues is perhaps best exemplified by axons crossing the ventral midline of the spinal cord (Colamarino and Tessier-Lavigne, 1995). In this paradigm, axons of commissural neurons in the dorsal spinal cord are initially attracted ventrally by long-range gradients of Netrin and Shh secreted from the floor plate, a specialized structure localized in the ventral spinal cord. Once commissural axons invade the floor plate, their sensitivity to attractive cues is silenced and axons are repelled to the contralateral side by floor plate-derived repulsive cues, including Slits and Sema3B (Chedotal, 2011). Thus, intermediate targets such as the floor plate express precise patterns of attractive and repulsive cues that function at long and short distances to orchestrate growth cone steering events that underlie the establishment of accurate axonal trajectories.

How precisely patterned gradients of secreted guidance cues form *in vivo* is not well understood, although components of the extracellular matrix (ECM) are likely to play an essential role. In principle, components of the ECM can influence interactions between secreted cues and their receptors in several ways, including controlling cue diffusion, concentrating cues in particular locales, affecting ligand-receptor binding affinity, modulating ligand or receptor processing, or influencing ligand stability (Lee and Chien, 2004; Muller and Schier, 2011). In *Drosophila,* ECM components have well-established roles in generating gradients of secreted morphogens *in vivo* (Yan and Lin, 2009). Furthermore, the localization of Slit is regulated by the proteoglycan syndecan in *Drosophila* and the ECM protein Collagen IV in zebrafish (Johnson et al., 2004; Xiao et al., 2011). How specific ECM components affect guidance cue distribution and function *in vivo* in the developing mammalian nervous system is largely unknown.

Using a forward genetic screen in mice, we have identified two genes, *β-1,3-N-acetyl-glucosaminyltransferase-1* (*B3gnt1*) and *Isoprenoid synthase domain containing* (*ISPD*), as novel regulators of axon guidance. We show that B3gnt1 and ISPD are essential for glycosylation of the extracellular matrix protein dystroglycan *in vivo*, and that *B3gnt1* and *ISPD* mutants develop severe neuronal migration defects commonly associated with defective dystroglycan function. We find that dystroglycan is also required for spinal cord basement membrane integrity, and that axon tracts growing in close proximity to the basement membrane are severely disorganized in *B3gnt1*, *ISPD*, and *dystroglycan* mutants. Remarkably, we find that glycosylated dystroglycan also binds directly to the axon guidance cue Slit to organize its protein distribution in the floor plate and the basement membrane, thereby regulating Slit-mediated axon guidance. These findings reveal a fundamental role for dystroglycan in organizing axon guidance cue distribution and function within the ECM and identify novel mechanisms underlying human pathologies.

Results

A forward genetic screen identifies B3gnt1, ISPD, and dystroglycan as novel regulators of axon guidance

We conducted an ENU-based, three-generation, forward genetic screen in order to identify novel mutations that affect the organization of PNS and CNS axonal tracts (Merte et al., 2010)(Figure S1). Utilizing a recessive breeding strategy, axonal tracts of E11.5–12.5 embryos were visualized using a wholemount anti-neurofilament based assay (Figure 1A). Screening of 235 G1 mouse lines led to the identification of 10 distinct lines harboring mutations resulting in axon guidance and axon branching defects (Figure 1B, E, data not shown).

Lines 1157 and 9445 were initially identified based on similar defects in the development of longitudinal axonal tracts in the hindbrain. In control embryos, axons emanating from the midbrain and cranial nerves project caudally to cervical levels of the spinal cord, forming a tightly fasciculated axon bundle that passes through the hindbrain. In line 1157 mutant embryos, these projections were truncated and defasciculated at the level of the vagal complex (Figure 1B). Line 9445 mutants showed a more severe phenotype, with the descending projections failing to project through the hindbrain altogether, and the central projections of the vagal complex projecting aberrantly within the hindbrain (Figure 1B).

Genetic mapping localized the mutation in line 1157 to a gene dense 6.5 Mb region on Chromosome 19. Targeted exon capture coupled with next-generation sequencing was used to sequence the coding exons within this region of interest. Of the 255 genes sequenced, we identified a single mutation, a T to C transversion in exon 1 of *β-1,3-N-Acetylglucosaminyltransferase 1* (*B3gnt1*), which results in a methionine to threonine (M155T) substitution in the B3gnt1 amino acid sequence (Figure 1C). *B3gnt1* encodes a glycosyltransferase, and the M155T mutation in B3gnt1 lies within the N-terminal portion of the catalytic domain (Figure 1C). Expression of myc-B3gnt1 in COS7 cells shows that this protein normally localizes to the Golgi apparatus (Figure S2A, top panels). In contrast, myc-B3gnt1^{M155T} is not localized to the Golgi but shows a high degree of overlap with the endoplasmic reticulum marker PDI (Figure S2A–B, bottom panels), suggesting it is misfolded and retained in the ER. To verify that the B3gnt1^{M155T} mutation causes the axon guidance phenotype in line 1157 mutants, we generated a targeted knockout mouse line in which the *B3gnt1* coding sequences were replaced with *LacZ* (*B3gnt1*^{LacZ}). Genetic complementation experiments showed that transheterozygous *B3gnt1*$^{LacZ/M155T}$ mice exhibit axon defasciculation in the descending hindbrain projections (data not shown), confirming that the mutation in *B3gnt1* is indeed the cause of the axon guidance defects observed in line 1157.

Genetic mapping of line 9445 localized the mutation to a 4.3 Mb region on Chromosome 12 that contains 18 genes. PCR amplification and sequencing of the coding exons of all 18 genes identified a single mutation, a T to A transversion, in exon 1 of the gene *Isoprenoid Synthase Domain Containing* (*ISPD*), which results in a conversion of a leucine to a premature stop codon (L79*) (Figure 1D). *ISPD* encodes a protein with homology to the bacterial protein IspD, a cytidyltransferase that functions in the methylerythritol phosphate (MEP) pathway of isoprenoid synthesis, which is not present in vertebrates (Richard et al., 2004).

Further analysis of the axon guidance phenotypes of *B3gnt1*$^{LacZ/M155T}$ and *ISPD*$^{L79*/L79*}$ embryos identified defects in the formation of the dorsal funiculus by the central projections of dorsal root ganglia (DRG) sensory neurons. In control embryos, the dorsal funiculus forms along the dorsal aspect of the spinal cord as a tightly fasciculated bundle. In contrast,

the dorsal funiculus in both *B3gnt1*$^{LacZ/M155T}$ and *ISPD*$^{L79*/L79*}$ mutants is highly defasciculated and exhibits a patchy and discontinuous appearance (Figure 1E).

The phenotypic similarities between the *B3gnt1* and *ISPD* mutants raised the intriguing possibility that they function in the same genetic pathway to regulate axon guidance. B3gnt1 has been implicated as a dystroglycan glycosyltransferase in tumor cell lines *in vitro* (Bao et al., 2009), and mutations in ISPD were recently identified in patients with Walker-Warburg syndrome, a neurodevelopmental disorder characterized by defective glycosylation of dystroglycan (Roscioli et al., 2012; Willer et al., 2012). While dystroglycan is known to be required for neuronal migration in the brain, it has not previously been implicated in regulating axon guidance. To determine if the axon guidance defects observed in *B3gnt1* and *ISPD* mutants are due to defects in dystroglycan function, we generated mice in which dystroglycan was deleted from the epiblast (*Sox2*^{cre}*; DG*$^{F/-}$) to circumvent the early embryonic lethality associated with germline deletion of dystroglycan. Indeed, *Sox2*^{cre}*; DG*$^{F/-}$ mice exhibit the same axon guidance defects as *B3gnt1* and *ISPD* mutants, with abnormal formation of the descending hindbrain axonal tract and severe defasciculation of the spinal cord dorsal funiculus (Figure 1B, E). These findings thus reveal a requirement for dystroglycan in regulating axon guidance.

B3gnt1 and *ISPD* mutants are novel mouse models of dystroglycanopathy

Dystroglycan functions *in vivo* in the assembly and maintenance of basement membranes by acting as a receptor and scaffold for several ECM proteins (Barresi and Campbell, 2006). Dystroglycan undergoes extensive glycosylation *in vivo*, and ligand binding to dystroglycan is strictly dependent on its proper glycosylation. Importantly, human patients with mutations in dystroglycan or its glycosyltransferases develop a spectrum of congenital muscular dystrophies that are often accompanied by a range of neurological defects. These disorders are collectively referred to as dystroglycanopathies, and their pathological hallmarks are recapitulated in mouse models with deletions in orthologous genes (Hewitt, 2009; Moore et al., 2002; Satz et al., 2008). Interestingly, several studies indicate that the majority of human patients with pathological defects in dystroglycan glycosylation have mutations of unknown etiology, suggesting that additional unknown glycosyltransferases are required for dystroglycan function *in vivo* (Mercuri et al., 2009).

While *B3gnt1*$^{M155T/M155T}$ mice are born at normal Mendelian ratios and display a mild muscular dystrophy phenotype of variable penetrance, *B3gnt1*$^{LacZ/LacZ}$ embryos failed to survive beyond E9.5, indicating that B3gnt1 is required for normal embryonic development and that the M155T mutation generates a hypomorphic allele. *B3gnt1*$^{LacZ/LacZ}$ early embryonic lethality is consistent with a role for B3gnt1 in regulating dystroglycan glycosylation and function *in vivo*, since mice deficient for dystroglycan die around E7.5 due to defects in Reichert's membrane, the basement membrane situated between the trophoblast and parietal endoderm cells of early mammalian embryos (Williamson et al., 1997). To circumvent *B3gnt1*$^{LacZ/LacZ}$ early embryonic lethality, we conducted all subsequent analyses using *B3gnt1*$^{LacZ/M155T}$ mice. The majority of *B3gnt1*$^{LacZ/M155T}$ mice die perinatally, but the few that do survive to adulthood develop symptoms characteristic of congenital muscular dystrophy, displaying a hunched posture, hindlimb clasping, and atrophic musculature (Figure S3A, B). Immunostaining of skeletal muscle from *B3gnt1*$^{LacZ/M155T}$ mice shows severe hypoglycosylation of dystroglycan (Figure S3C), and examination of membrane-enriched extracts isolated from *B3gnt1*$^{LacZ/M155T}$ skeletal muscle revealed that glycosylated alpha-dystroglycan is reduced to a nearly undetectable amount, while the level of total dystroglycan protein is normal (Figure S3D). Consistent with the inability of hypoglycosylated dystroglycan to bind ligand, extracts from *B3gnt1*$^{LacZ/M155T}$ mice are deficient for laminin binding (Figure S3D).

While a complete loss of *B3gnt1* results in early embryonic lethality, $ISPD^{L79*/L79*}$ embryos were obtained at normal Mendelian ratios up to E18, suggesting that ISPD function is not required for formation of Reichert's membrane. However, all $ISPD^{L79*/L79*}$ mutants that were born died at P0 due to apparent respiratory failure, preventing any analysis of a muscular dystrophy phenotype.

In the central nervous system, deletion of dystroglycan or its glycosyltransferases results in neuronal migration defects similar to type II (cobblestone) lissencephaly. Examination of membrane-enriched extracts from $B3gnt1^{LacZ/M155T}$ and $ISPD^{L79*/L79*}$ brains revealed that while the levels of total dystroglycan protein are normal, glycosylated alpha-dystroglycan and laminin binding activity are reduced to an undetectable amount (Figure 2A, B). In the cortex of control embryos, glycosylated dystroglycan expression is enriched in radial glial endfeet where it binds to extracellular matrix proteins to organize and maintain the basement membrane along the basal cortical surface (Figure 2C). In the cortex of $B3gnt1^{LacZ/M155T}$ and $ISPD^{L79*/L79*}$ mice, dystroglycan glycosylation is lost, leading to a loss of laminin accumulation in the basement membrane (Figure 2C). Previous analysis of mice in which dystroglycan was conditionally deleted from radial glia observed neuronal migration defects in regions where radial glia endfeet had detached from the basement membrane (Satz et al., 2010). $B3gnt1^{LacZ/M155T}$ and $ISPD^{L79*/L79*}$ mice show similar migration defects in the cortex, exhibiting radial glial endfoot detachment and neuronal heterotopias similar to those found in cobblestone lissencephaly (Figure 2C, S4A, data not shown). Analysis of surviving adult $B3gnt1^{LacZ/M155T}$ mice showed that they also exhibit neuronal migration defects in the cerebellum and hippocampus and develop hydrocephaly (Figure S4B, data not shown). Taken together, these defects confirm that B3gnt1 and ISPD function in the same genetic pathway to regulate dystroglycan glycosylation *in vivo*, and establish $B3gnt1^{LacZ/M155T}$ and $ISPD^{L79*/L79*}$ mice as novel mouse models of dystroglycanopathy.

Dystroglycan is required for basement membrane integrity in the developing spinal cord

The axon guidance defects observed in *B3gnt1*, *ISPD* and *dystroglycan* mutants suggests a novel role for dystroglycan *in vivo*. The axons of both the descending hindbrain projections and the dorsal funiculus extend along the basal surface of the hindbrain and spinal cord, respectively, suggesting that dystroglycan may be required in the hindbrain and spinal cord for the proper development of these axonal tracts. In contrast to the well-characterized role of dystroglycan in the developing cortex, its function in the spinal cord is unclear. Similar to the developing cortex, levels of total dystroglycan protein in the spinal cord of $B3gnt1^{LacZ/M155T}$ and $ISPD^{L79*/L79*}$ mutants are normal, while glycosylated alpha-dystroglycan and laminin binding activity are reduced to an undetectable amount (Figure 3A, B). Examination of dystroglycan localization by immunostaining shows that dystroglycan is enriched in the radial neuroepithelial endfeet, where it co-localizes with several extracellular matrix proteins including laminin, perlecan, and collagen IV to form a continuous basement membrane surrounding the spinal cord (Figure 3C, S5A). In $B3gnt1^{LacZ/M155T}$, $ISPD^{L79*/L79*}$ and $Sox2^{cre};DG^{F/-}$ embryos, the loss of functional dystroglycan results in the progressive fragmentation of the basement membrane beginning around E11.5 which is accompanied by detachment of radial neuroepithelial endfeet from the basal surface (Figure S5A, S5B). This fragmentation first appears in the lateral portion of the spinal cord, and progresses ventrally and dorsally as the spinal cord continues to develop.

Dystroglycan is required for commissural axon crossing in the spinal cord

Interestingly, in addition to its localization to the basement membrane surrounding the spinal cord, we found that dystroglycan is enriched in the floor plate, a specialized glial structure in the ventral neuraxis that spans the CNS anteroposterior axis from the midbrain to caudal

spinal cord (Figure 3C, D). The spinal cord floor plate functions both as an organizer of ventral cell fates and as an intermediate target for commissural axons whose cell bodies reside within the dorsal spinal cord. The axons of commissural neurons are initially attracted ventrally to the floor plate by a number of floor plate derived cues, including Netrin, Shh, and VEGF (Charron et al., 2003; Ruiz de Almodovar et al., 2011; Serafini et al., 1996). Once commissural axons reach the floor plate, these attractive cues are silenced and repulsive floor plate-derived cues, including Slits (Long et al., 2004) and Sema3B (Zou et al., 2000), force axons out of the floor plate and into the contralateral side of the spinal cord, where they turn rostrally and extend in close proximity to the basement membrane to form the ventrolateral funiculus.

Since enrichment of dystroglycan in the floor plate is similar to Slit and other axon guidance cues, we hypothesized that dystroglycan regulates guidance of commissural axons as they cross the ventral midline. Analysis at E11.5, a time when axons are beginning to project through the floor plate, revealed minor disruptions in the glial structures and the basement membrane within the floor plate in the absence of dystroglycan (Figure S5B). In control E11.5 embryos, commissural axons labeled with an antibody to L1 project through the floor plate and turn rostrally, forming the ventrolateral funiculus (Figure 4A–D). In contrast, commissural axons in $B3gnt1^{LacZ/M155T}$, $ISPD^{L79*/L79*}$, and $Sox2^{Cre};DG^{F/-}$ mutant embryos exhibit robust post-crossing trajectory defects (Figure 4A–D). These axons fail to project to the lateral portion of the funiculus, and quantification revealed that the ratio of the areas occupied by the lateral and ventral funiculi is significantly altered in $B3gnt1^{LacZ/M155T}$, $ISPD^{L79*/L79*}$, and $Sox2^{Cre};DG^{F/-}$ embryos (Figure 4E). This failure of post-crossing commissural axons to project into the lateral portion of the funiculus is remarkably similar to the phenotype observed in *Robo1/2* knockout mice (Figure 4D, E) (Jaworski et al., 2010). Analysis of post-crossing commissural axons two days later at E13.5 found that in addition to the lateral-to-ventral shift in axonal trajectory, *B3gnt1* and *dystroglycan* mutants also exhibit extensive disruptions in the more lateral aspect of the ventrolateral funiculus as axons project along the basement membrane, a phenotype that is not observed in control or *Robo1/2* mutants (Figure S6A–D).

Examination of the floor plate in E13 $B3gnt1^{LacZ/M155T}$, $ISPD^{L79*/L79*}$ and $Sox2^{Cre};DG^{F/-}$ embryos at higher magnification revealed a large number of commissural axons projecting abnormally within the floor plate (Figure 5A, arrows). To better characterize the nature of these commissural axon misprojections, we used DiI labeling in an open-book preparation to unilaterally label small populations of commissural neurons and their axonal projections (Long et al., 2004). In control embryos, commissural axons were observed crossing the floor plate (dashed lines) and turning rostrally after exiting the floor plate (Figure 5B). In stark contrast, many commissural axons in $B3gnt1^{LacZ/M155T}$, $ISPD^{L79*/L79*}$ and $Sox2^{Cre};DG^{F/-}$ embryos stalled within the floor plate. The axons that did exit the floor plate showed abnormal turning behaviors, exhibiting random turning (extending either rostrally and caudally) and/or failing to turn at all (Figure 5B). Quantification of commissural axon turning behaviors at several different axial levels of the spinal cord showed that axons in greater than 80% of DiI labeled sites in control embryos turn rostrally after floor plate crossing, whereas axons in fewer than 10% of DiI labeled sites exhibit this behavior in $B3gnt1^{LacZ/M155T}$, $ISPD^{L79*/L79}$ and $Sox2^{Cre};DG^{F/-}$ embryos. These findings establish an essential role for glycosylated dystroglycan in regulating axon guidance at the ventral midline of the spinal cord *in vivo*.

Dystroglycan binds Slit to regulate axon guidance in the floor plate

The commissural axon guidance phenotypes observed in the *B3gnt1, ISPD* and *dystroglycan* mutants raised the possibility that dystroglycan binds to axon guidance cues within the floor plate to regulate their function. Previous studies have identified a number of ligands that

bind directly to dystroglycan in a glycosylation-dependent manner, including laminin, agrin, perlecan, neurexin, and pikachurin (Gee et al., 1994; Sato et al., 2008; Sugita et al., 2001; Talts et al., 1999). A common feature of these ligands is the presence of a laminin G (LG) domain that mediates their association with carbohydrate moieties present on glycosylated dystroglycan. Intriguingly, of the axon guidance cues known to be expressed in the floor plate, Slits contain an LG domain within their C-terminal regions. Thus, the overlapping expression patterns of *dystroglycan* and *Slits* in the floor plate, the similarities in axon guidance phenotypes observed in the *B3gnt1*, *ISPD*, *dystroglycan* and *Slit/Robo* mutants, and the presence of an LG domain in the Slit C-terminus, led us to hypothesize that glycosylated dystroglycan binds directly to Slits to regulate their function.

We first asked whether dystroglycan can bind directly to the C-terminal region of Slit, which harbors the LG domain, using an *in vitro* COS7 cell-binding assay. We generated constructs in which alkaline phosphatase (AP) is fused to either the Robo-binding leucine rich repeat domain 2 of Slit2 (AP-LRR) or the C-terminal region containing the LG domain of Slit2 (AP-Cterm). As expected, COS7 cells transfected with a construct encoding full-length Robo-1 specifically bind to AP-LRR, but not to AP-Cterm or AP alone (Figure 6A, data not shown). Importantly, COS7 cells expressing full-length dystroglycan showed robust binding to AP-Cterm but not to AP-LRR or AP alone. These findings demonstrate that dystroglycan is capable of binding to the Slit C-terminal domain. To further test direct binding between dystroglycan and Slit, we generated an Fc-dystroglycan protein secreted from COS7 cells and determined whether it is capable of direct association with the different domains of Slit. We find that while Fc-dystroglycan fails to bind to AP-LRR, it does bind to AP-Cterm (Figure 6B). We next asked whether the Slit C-terminal fragment is able to bind to endogenous dystroglycan. Dystroglycan enriched membrane fractions isolated by WGA precipitation from mouse brain lysates were incubated with either AP-LRR or AP-Cterm. Indeed, the Slit C-terminal fragment, but not the Slit LRR, is able to associate with endogenous dystroglycan (Figure 6C).

Previous studies indicate that the binding of laminin LG domains to dystroglycan requires a basic patch surrounding a Ca^{2+} binding site (Harrison et al., 2007). Alignment of the Slit2 LG domain with the known structure of laminin α1 LG5 identified a putative Ca^{2+} binding site surrounded by several basic residues (Figure 6D). We found that binding of the Slit C-terminal domain to dystroglycan requires Ca^{2+}, since addition of EDTA is sufficient to abolish this Slit–dystroglycan interaction (Figure 6E). Moreover, a version of the Slit2 C-terminal domain in which two basic residues adjacent to the Ca^{2+} binding site are mutated to alanine (K1177A, R1179A, referred to here as Slit2 C-term AVA) is incapable of binding to Fc-dystroglycan (Figure 6F). Thus, the Slit2 LG domain mediates its association with dystroglycan and, similar to other LG modules, the Slit2 LG domain requires a Ca^{2+} binding site surrounded by a basic patch for this interaction.

Our findings that Slit can bind directly to dystroglycan *in vitro* raise the intriguing possibility that dystroglycan present in the floor plate and basement membrane serves as a scaffold for the proper localization of Slit *in vivo*. Consistent with this idea, *dystroglycan* and *slit* are required for proper cardiac tube formation in *Drosophila*, and Slit protein appears to be mislocalized in *dystroglycan* mutant cardioblasts (Medioni et al., 2008). We first verified that the expression patterns of *Slit1* and *Slit2* mRNA are indistinguishable in control and *B3gnt1* mutants (Figure S7A), demonstrating that dystroglycan is not required for floor plate development or expression of these axonal guidance cues. To test whether dystroglycan regulates Slit localization, an AP-section binding assay was employed to visualize the location of endogenous C-terminal Slit binding sites *in vivo*. Incubation of transverse spinal cord sections from E11 control embryos with the AP-Slit C-term ligand showed robust binding to the basement membrane surrounding the spinal cord and the floor

plate (Figure 7A), regions that are enriched for dystroglycan protein expression (Figure 3C, D). Importantly, binding of AP-Slit C-term is absent in *B3gnt1*$^{LacZ/M115T}$ mutants, demonstrating that glycosylation of dystroglycan is essential for Slit C-terminal domain binding *in vivo*.

Since Slit binds directly to glycosylated dystroglycan *via* its C-terminal LG domain, we hypothesized that dystroglycan present in both the floor plate and basement membrane are required for organization of endogenous Slit proteins within these locations. Therefore, we developed a method to assess the sites of Slit protein localization in tissue sections to ask whether loss of glycosylated dystroglycan in the *B3gnt1* mutants alters the distribution of endogenous Slit protein *in vivo*. The lack of antibodies suitable for mammalian Slit immunolocalization necessitated the development of an alternate approach. Therefore, we modified the AP-ligand section binding assay by using an AP-Robo ectodomain fusion protein that is capable of binding to Slit protein on tissue sections (Jaworski and Tessier-Lavigne, 2012). AP-Robo bound specifically in the floor plate and in close proximity to the ventrolateral funiculus formed by post-crossing commissural axons (Figure 7B). In contrast, AP-Robo binding sites are strikingly deficient in both the floor plate and ventrolateral funiculus in sections from *B3gnt1* mutants. These findings demonstrate that the *in vivo* distribution of endogenous Slit protein is dependent upon glycosylated dystroglycan, providing an explanation for the Slit/Robo-like phenotypes in *B3gnt1*, *ISPD* and *dystroglycan* mutants and therefore insight into the mechanistic basis underlying axon guidance defects in mice, and presumably humans, with dystroglycanopathies.

Discussion

We report here that B3gnt1 and ISPD are required for dystroglycan glycosylation *in vivo*, and that glycosylated dystroglycan is required for proper guidance and development of several axonal tracts. We identified two mechanisms by which dystroglycan regulates axon guidance. First, dystroglycan is required for the integrity of basement membranes that developing axonal tracts extend along, thereby maintaining a permissive growth environment. Second, we found that dystroglycan binds directly to the laminin G domain of Slit, thereby organizing Slit protein distribution *in vivo*. Therefore, dystroglycan likely functions as an extracellular scaffold that controls axon guidance events by organizing the availability of axonal growth and guidance cues at critical intermediate targets. Furthermore, our findings suggest that misregulation of Slit–Robo signaling contributes to axonal guidance and neuronal connectivity defects in human patients with dystroglycanopathies.

B3gnt1 and *ISPD* mutants are novel models of dystroglycanopathy

Glycosylated dystroglycan is required for the organization of ECM proteins in basement membranes. Mutations that disrupt glycosylation of dystroglycan and result in dystroglycanopthies in humans have been identified in seven genes: *POMT1*, *POMT2*, *POMGnt1*, *Fukutin*, *FKRP*, *LARGE,* and recently *ISPD* (Hewitt, 2009; Roscioli et al., 2012; Willer et al., 2012). However, the molecular etiology of many patients with dystroglycanopthies is unknown, suggesting that additional unidentified genes are required for dystroglycan glycosylation (Mercuri et al., 2009). Through our forward genetic screen in mice we identified *B3gnt1* and *ISPD* mutants as novel mouse models for dystroglycanopathy.

Genetic and biochemical findings demonstrate extensive heterogeneity in the glycosylation of dystroglycan which, although it has a predicted molecular mass of 72 kD, exhibits an apparent molecular mass that ranges from 120kD in cortex and peripheral nerve to 160kD in skeletal muscle and 180kD in the cerebellar Purkinje neurons (Satz et al., 2010). While this heterogeneity has made the precise composition of the glycan sidechains on dystroglycan

difficult to ascertain, dystroglycan isolated from mouse brain contains both *O*-GalNAc- and *O*-Mannose-initiated glycan side chains that require POMT1, POMT2, and POMGnt1 for their synthesis (Stalnaker et al., 2011). Recent studies indicate that LARGE functions as both a bifunctional xylosyltransferase and glucuronyltransferase (Inamori et al., 2012), while the enzymatic functions of Fukutin and FKRP have yet to be elucidated. Likewise, the enzymatic steps catalyzed by B3gnt1 and ISPD in the production of mature, fully glycosylated dystroglycan is presently unknown. The *B3gnt1* and *ISPD* mutant mice should provide useful tools for resolving this issue. Interestingly, analysis of the subcellular localization of Fukutin revealed that while the wildtype protein localizes to the Golgi, several disease-causing missense mutations in *Fukutin* result in a protein that is aberrantly localized to the ER (Tachikawa et al., 2012). Similarly, while wildtype B3gnt1 is associated with the Golgi, the M155T mutation results in B3gnt1 mislocalization to the ER, suggesting that this missense mutation may result in improper folding of B3gnt1 leading to its impaired function *in vivo* (Figure S2).

It is interesting to note that although we were unable to detect any glycosylated dystroglycan in *ISPD* mutants and these mutants appeared to fully phenocopy $Sox2^{cre}; DG^{F/-}$ mutants, *ISPD* mutants were able to survive until birth, strongly suggesting that ISPD function is not required for formation of Reichert's membrane. This is unique among genes required for dystroglycan glycosylation, as complete loss-of-function mutations in these genes, with the exception of *POMGnt1*, leads to loss of Reichert's membrane and early embryonic lethality.

Dystroglycan is a novel regulator of Slit–Robo signaling and axon guidance

Dystroglycan has a well-characterized role in regulating neuronal migration in the developing brain since it is required for radial glia endfoot attachment to the basement membrane surrounding the brain. Our analysis of *B3gnt1*, *ISPD* and *dystroglycan* mutant mice reveals an additional, critical role for dystroglycan in the development of several axonal tracts.

The prevailing model for axon guidance at the spinal cord floor plate posits that axons are initially attracted to the floor plate by long-range gradients of the chemoattractants Netrin and Shh, and attraction is silenced and converted to repulsion once axons reach the floor plate. Thus, precise spatial and temporal Slit expression patterns are essential for proper commissural axon midline crossing. The spinal cord commissural axon crossing phenotypes observed in the *B3gnt1, ISPD* and *dystroglycan* mutants prompted us to ask whether glycosylated dystroglycan regulates axon guidance at the ventral midline *via* modulation of floor plate derived guidance cues. Indeed, we found that dystroglycan binds directly to the laminin G domain in the C-terminal portion of Slit and that this interaction is required for the localization of Slit protein at the floor plate where it guides commissural axons across the midline. While there are differences in the axon guidance phenotypes between the *B3gnt1*, *ISPD* and *dystroglycan* mutants and the *Slit* or *Robo* mutants, we would not anticipate precisely the same phenotypes, as our model posits that the loss of functional dystroglycan results in a mislocalization of Slit from the floor plate and basement membranes, as opposed to a complete loss of Slit-Robo signaling. Indeed, the randomization of anterior-posterior post-crossing trajectories observed in *B3gnt1, ISPD* and *dystroglycan* mutants has not been reported in either *Slit* or *Robo* mutants, but is seen in *Sema3B/Npn2/Plexin-A1* and *Wnt4/Fzd3* mutants (Lyuksyutova et al., 2003; Nawabi et al., 2010; Zou et al., 2000), suggesting that dystroglycan may organize additional floor plate or basement membrane-associated axon guidance cues. Interestingly, consistent with our observation of axonal guidance defects in *B3gnt1, ISPD* and *dystroglycan* mutants, postmortem analysis of a patient with Walker-Warburg Syndrome, a severe form of dystroglycanopathy, revealed a reduction of the spinal cord lateral funiculus (Kanoff et al., 1998). Together, these findings

suggest that defects in axon guidance cue signaling, including Slit–Robo signaling, are contributing factors in the pathology of human patients with dystroglycanopathies.

Basement membrane integrity is required for axon guidance

In addition to guiding axonal projections at the floor plate through interactions with Slit, we find that glycosylated dystroglycan controls axon guidance through a second, distinct mechanism: organization of basement membrane ECM components. Although the role of ECM proteins in regulating axonal growth and guidance has been well documented *in vitro*, an understanding of how these molecules regulate specific axon guidance events *in vivo* is lacking. In *Drosophila, Laminin A* is required for guidance of ocellar photoreceptor axons but not the neighboring mechanosensory bristle axons, demonstrating that different neuronal populations can have distinct ECM requirements for axonal guidance *in vivo* (Garcia-Alonso et al., 1996). Throughout the mammalian nervous system, glycosylated dystroglycan localized near the endfeet of radial neuroepithelial cells serves as an essential scaffold for ECM proteins, including laminin, perlecan and collagen IV, to form the basement membrane. The axons that form the dorsal funiculus, ventrolateral funiculus and descending hindbrain projections extend along the basal surface of the developing hindbrain and spinal cord, in direct apposition to the basement membrane (Figure S6E). The coincident disorganization of these axon tracts and the disruption of the basement membrane components laminin, perlecan, and collagen IV in *B3gnt1, ISPD* and *dystroglycan* mutants strongly suggests that development of these axonal projections requires dystroglycan to organize the ECM-rich basement membrane as a growth and guidance substrate. Recent work has also implicated the basement membrane in coordinating the localization of axon guidance cues, including draxin in the developing spinal cord (Islam et al., 2009) and collagen IV-dependent localization of Slit in the optic tectum (Xiao et al., 2011). Thus, ECM components of the basement membrane control proper growth and fasciculation of major axonal fiber tracts in the developing nervous system.

The modular structure of Slit provides a mechanism for spatial restriction

Slits have a modular domain structure, with an N-terminal domain containing the LRR regions required for Robo binding and, as shown here, a C-terminal domain that mediates direct association with dystroglycan. Slit proteins can be cleaved both *in vitro* and *in vivo*, with both full-length Slits and their N-terminal fragments exhibiting repulsive axon guidance activity, while the Slit C-terminal domains have no effect on axon repulsion *in vitro* (Brose et al., 1999; Nguyen Ba-Charvet et al., 2001). However, the functional relevance of Slit cleavage *in vivo* is unclear, as re-introduction of a non-cleavable form of Slit into *slit* mutant *Drosophila* is able to rescue axon guidance defects (Coleman et al., 2010). The modular structure of Slit is particularly interesting with respect to its interaction with heparan sulfate proteoglycans (HSPGs), which have a critical role in mediating Slit–Robo signaling both *in vitro* (Hu, 2001) and *in vivo* (Bulow et al., 2008; Inatani et al., 2003; Johnson et al., 2004; Pratt et al., 2006; Steigemann et al., 2004). Biochemical studies have identified a heparin binding site in the LRR region of the N-terminal portion of Slit that stabilizes its interaction with Robo, while a second high-affinity HS binding site is located in the C-terminal domain (Hussain et al., 2006). The functional significance of HSPG binding to the C-terminal portion of Slit is unknown, but one interesting possibility is that the Slit–HSPG interaction stabilizes the Slit C-terminal binding to dystroglycan, similar to the role of heparin in stabilizing the LRR–Robo interaction. These findings, taken together, reveal the modular nature of Slit proteins, with separable Robo and dystroglycan binding domains, and define a mechanism for establishing sites of ligand-receptor interactions that control axonal guidance decisions with great spatial fidelity.

In summary, we have identified B3gnt1 and ISPD as required for dystroglycan glycosylation and thus organization of ECM components *in vivo*. Our analysis of *B3gnt1, ISPD* and *dystroglycan* mutants reveals an essential role for glycosylated dystroglycan in the development of several major axonal tracts that grow along basement membranes, including the spinal cord ventrolateral funiculus, dorsal funiculus, and descending hindbrain projections. Dystroglycan binds directly to the C-terminal laminin G domain of the axon guidance cue Slit, and this interaction is essential for organizing Slit protein distribution in both the basement membrane and spinal cord floor plate and for the guidance of commissural axons. We propose that axonal guidance defects resulting from aberrant axonal guidance cue signaling, including aberrant Slit–Robo signaling, contribute to the pathology of human dystroglycanopathies.

Experimental Procedures

Forward genetic screen

The three-generation forward genetic screen and wholemount neurofilament staining assay were performed as described in detail (Merte et al., 2010).

Generation of B3gnt1^{LacZ} mice

B3gnt1^{LacZ} mice, in which the coding region of B3gnt1 was replaced with a *lacZ* cassette, were generated using C57BL/6 ES cells obtained from the trans-NIH Knockout Mouse Project (KOMP). Genotypic procedures are described in the supplemental experimental procedures.

Immunohistochemistry, *in situ* hybridization, and western blotting

Antibodies were used at the following dilutions: anti-IIH6 (1:100, Millipore), anti β-dystroglycan (1:100, Santa Cruz), 2H3 (1:3000, concentrated ascites, DSHB), anti-Nestin (1:100, DSHB) anti-L1 (1:250, Millipore), anti-Laminin (1:1000, Sigma), anti-Perlecan (1:500, Millipore), anti-Collagen IV (1:500, Southern Biotech). *In situ* hybridization was performed using standard procedures and the following probe for *dystroglycan* (nucleotodes 562-1034 of NM_010017). *Slit1* and *Slit2* probes were described previously (Yuan et al., 1999). Analysis of dystroglycan glycosylation and laminn binding activity in various tissues by western blotting was performed as described (Satz et al., 2010), and are detailed further in the supplemental experimental procedures.

DiI injections and L1 quantification in spinal cords

To label commissural axons at the floor plate, open book preparations from E13 embryos were unilaterally injected with DiI and imaged 16–24 hours later. The behavior of commissural axons was scored as normal, stalled, straight, or random (axons projecting both anteriorly and posteriorly following floor plate exit). For quantification of the ventrolateral funiculus area, the area occupied by L1 positive axons in the ventral funiculus and lateral funiculus was calculated using ImageJ using the motor exit point as the demarcation between ventral and lateral funiculi. Three different forelimb levels sections were quantified per animal, and at least three animals were used for each genotype.

Slit-Dystroglycan binding

To test binding between dystroglycan and Slit, COS7 cells were transfected with constructs encoding α-dystroglcyan-Fc (DG-Fc), AP alone, AP-Slit2 LRR, AP-Slit2 Cterm, or AP-Slit2 Cterm AVA. Secreted ligands were collected from the supernatant, concentrated, and dialyzed in binding buffer (50mM Tris-HCl, pH7.5, 150mM NaCl, 2.5 mM $MgCl_2$, 2.5 mM $CaCl_2$). For DG-Fc binding experiments, DG-Fc was incubated overnight with the indicated

ligands, then recovered by binding to protein A/G beads for two hours, washed five times in binding buffer, and eluted by boiling in sample buffer. For analysis of Slit binding to endogenous dystroglycan, Slit ligands were incubated overnight with WGA-enriched fractions isolated from mouse brain tissue that had been dialyzed overnight in binding buffer. Ligands contained a C-terminal 6xHis tag and were recovered by a two-hour incubation with Ni-NTA beads, washed five times in binding buffer, and eluted by boiling in sample buffer.

AP Binding Assays

For COS7 AP-binding, cells expressing either full-length dystroglycan or full-length Robo-1 were incubated with the indicated ligands. For AP-section binding, 50μm cryostat sections were incubated with the indicated ligands. Further details are provided in the supplemental experimental procedures.

Supplementary Material

Refer to Web version on PubMed Central for supplementary material.

Acknowledgments

We thank members of the Ginty laboratory for assistance and discussions throughout the course of this project, Christopher Walsh and Chiara Manzini for insightful comments, and Randal Hand, Alex Kolodkin, Seth Margolis, Martin Riccomagno, Sarah Sarsfield, and Megan Straiko for comments on the manuscript. We thank Kevin Campbell and Alain Chedotal for providing DNA constructs. The 2H3 and Nestin monoclonal antibodies were obtained from the Developmental Studies Hybridoma Bank developed under the auspices of the NICHD and maintained by The University of Iowa, Department of Biology, Iowa City, IA 52242. This work was supported by NIH grants NS34814 (DDG), NS062047 (LM), and R01HD055545 (DJL), and the Johns Hopkins Brain Sciences Institute (DDG). DDG is an investigator of the Howard Hughes Medical Institute.

References

Bao X, Kobayashi M, Hatakeyama S, Angata K, Gullberg D, Nakayama J, Fukuda MN, Fukuda M. Tumor suppressor function of laminin-binding alpha-dystroglycan requires a distinct beta3-N-acetylglucosaminyltransferase. Proceedings of the National Academy of Sciences. 2009; 106:12109–12114.

Barresi R, Campbell KP. Dystroglycan: from biosynthesis to pathogenesis of human disease. Journal of Cell Science. 2006; 119:199–207. [PubMed: 16410545]

Brose K, Bland KS, Wang KH, Arnott D, Henzel W, Goodman CS, Tessier-Lavigne M, Kidd T. Slit proteins bind Robo receptors and have an evolutionarily conserved role in repulsive axon guidance. Cell. 1999; 96:795–806. [PubMed: 10102268]

Bulow HE, Tjoe N, Townley RA, Didiano D, van Kuppevelt TH, Hobert O. Extracellular sugar modifications provide instructive and cell-specific information for axon-guidance choices. Current Biology. 2008; 18:1978–1985. [PubMed: 19062279]

Charron F, Stein E, Jeong J, McMahon AP, Tessier-Lavigne M. The morphogen sonic hedgehog is an axonal chemoattractant that collaborates with netrin-1 in midline axon guidance. Cell. 2003; 113:11–23. [PubMed: 12679031]

Chedotal A. Further tales of the midline. Current Opinion in Neurobiology. 2011; 21:68–75. [PubMed: 20724139]

Colamarino SA, Tessier-Lavigne M. The role of the floor plate in axon guidance. Annual Review of Neuroscience. 1995; 18:497–529.

Coleman HA, Labrador JP, Chance RK, Bashaw GJ. The Adam family metalloprotease Kuzbanian regulates the cleavage of the roundabout receptor to control axon repulsion at the midline. Development. 2010; 137:2417–2426. [PubMed: 20570941]

Engle EC. Human genetic disorders of axon guidance. Cold Spring Harbor Perspectives in Biology. 2010; 2:a001784. [PubMed: 20300212]

Garcia-Alonso L, Fetter RD, Goodman CS. Genetic analysis of Laminin A in Drosophila: extracellular matrix containing laminin A is required for ocellar axon pathfinding. Development. 1996; 122:2611–2621. [PubMed: 8787736]

Garel S, Rubenstein JL. Intermediate targets in formation of topographic projections: inputs from the thalamocortical system. Trends in Neurosciences. 2004; 27:533–539. [PubMed: 15331235]

Gee SH, Montanaro F, Lindenbaum MH, Carbonetto S. Dystroglycan-alpha, a dystrophin-associated glycoprotein, is a functional agrin receptor. Cell. 1994; 77:675–686. [PubMed: 8205617]

Harrison D, Hussain SA, Combs AC, Ervasti JM, Yurchenco PD, Hohenester E. Crystal structure and cell surface anchorage sites of laminin alpha1LG4-5. The Journal of Biological Chemistry. 2007; 282:11573–11581. [PubMed: 17307732]

Hewitt JE. Abnormal glycosylation of dystroglycan in human genetic disease. Biochimica et Biophysica Acta. 2009; 1792:853–861. [PubMed: 19539754]

Hu H. Cell-surface heparan sulfate is involved in the repulsive guidance activities of Slit2 protein. Nature Neuroscience. 2001; 4:695–701.

Hussain SA, Piper M, Fukuhara N, Strochlic L, Cho G, Howitt JA, Ahmed Y, Powell AK, Turnbull JE, Holt CE, et al. A molecular mechanism for the heparan sulfate dependence of slit-robo signaling. The Journal of Biological Chemistry. 2006; 281:39693–39698. [PubMed: 17062560]

Inamori K, Yoshida-Moriguchi T, Hara Y, Anderson ME, Yu L, Campbell KP. Dystroglycan function requires xylosyl- and glucuronyltransferase activities of LARGE. Science. 2012; 335:93–96. [PubMed: 22223806]

Inatani M, Irie F, Plump AS, Tessier-Lavigne M, Yamaguchi Y. Mammalian brain morphogenesis and midline axon guidance require heparan sulfate. Science. 2003; 302:1044–1046. [PubMed: 14605369]

Islam SM, Shinmyo Y, Okafuji T, Su Y, Naser IB, Ahmed G, Zhang S, Chen S, Ohta K, Kiyonari H, et al. Draxin, a repulsive guidance protein for spinal cord and forebrain commissures. Science. 2009; 323:388–393. [PubMed: 19150847]

Jaworski A, Long H, Tessier-Lavigne M. Collaborative and specialized functions of Robo1 and Robo2 in spinal commissural axon guidance. The Journal of Neuroscience. 2010; 30:9445–9453. [PubMed: 20631173]

Jaworski A, Tessier-Lavigne M. Autocrine/juxtaparacrine regulation of axon fasciculation by Slit-Robo signaling. Nature Neuroscience. 2012; 15:367–369.

Johnson KG, Ghose A, Epstein E, Lincecum J, O'Connor MB, Van Vactor D. Axonal heparan sulfate proteoglycans regulate the distribution and efficiency of the repellent slit during midline axon guidance. Current Biology. 2004; 14:499–504. [PubMed: 15043815]

Kanoff RJ, Curless RG, Petito C, Falcone S, Siatkowski RM, Pegoraro E. Walker-Warburg syndrome: neurologic features and muscle membrane structure. Pediatric Neurology. 1998; 18:76–80. [PubMed: 9492098]

Kolodkin AL, Tessier-Lavigne M. Mechanisms and molecules of neuronal wiring: a primer. Cold Spring Harbor Perspectives in Biology. 2011:3.

Lee JS, Chien CB. When sugars guide axons: insights from heparan sulphate proteoglycan mutants. Nature Reviews Genetics. 2004; 5:923–935.

Long H, Sabatier C, Ma L, Plump A, Yuan W, Ornitz DM, Tamada A, Murakami F, Goodman CS, Tessier-Lavigne M. Conserved roles for Slit and Robo proteins in midline commissural axon guidance. Neuron. 2004; 42:213–223. [PubMed: 15091338]

Lyuksyutova AI, Lu CC, Milanesio N, King LA, Guo N, Wang Y, Nathans J, Tessier-Lavigne M, Zou Y. Anterior-posterior guidance of commissural axons by Wnt-frizzled signaling. Science. 2003; 302:1984–1988. [PubMed: 14671310]

Medioni C, Astier M, Zmojdzian M, Jagla K, Semeriva M. Genetic control of cell morphogenesis during Drosophila melanogaster cardiac tube formation. The Journal of Cell Biology. 2008; 182:249–261. [PubMed: 18663140]

Mercuri E, Messina S, Bruno C, Mora M, Pegoraro E, Comi GP, D'Amico A, Aiello C, Biancheri R, Berardinelli A, et al. Congenital muscular dystrophies with defective glycosylation of dystroglycan: a population study. Neurology. 2009; 72:1802–1809. [PubMed: 19299310]

Merte J, Wang Q, Vander Kooi CW, Sarsfield S, Leahy DJ, Kolodkin AL, Ginty DD. A forward genetic screen in mice identifies Sema3A(K108N), which binds to neuropilin-1 but cannot signal. The Journal of Neuroscience. 2010; 30:5767–5775. [PubMed: 20410128]

Moore SA, Saito F, Chen J, Michele DE, Henry MD, Messing A, Cohn RD, Ross-Barta SE, Westra S, Williamson RA, et al. Deletion of brain dystroglycan recapitulates aspects of congenital muscular dystrophy. Nature. 2002; 418:422–425. [PubMed: 12140559]

Muller P, Schier AF. Extracellular movement of signaling molecules. Developmental Cell. 2011; 21:145–158. [PubMed: 21763615]

Nawabi H, Briancon-Marjollet A, Clark C, Sanyas I, Takamatsu H, Okuno T, Kumanogoh A, Bozon M, Takeshima K, Yoshida Y, et al. A midline switch of receptor processing regulates commissural axon guidance in vertebrates. Genes & Development. 2010; 24:396–410. [PubMed: 20159958]

Nguyen Ba-Charvet KT, Brose K, Ma L, Wang KH, Marillat V, Sotelo C, Tessier-Lavigne M, Chedotal A. Diversity and specificity of actions of Slit2 proteolytic fragments in axon guidance. The Journal of Neuroscience. 2001; 21:4281–4289. [PubMed: 11404413]

Pratt T, Conway CD, Tian NM, Price DJ, Mason JO. Heparan sulphation patterns generated by specific heparan sulfotransferase enzymes direct distinct aspects of retinal axon guidance at the optic chiasm. The Journal of Neuroscience. 2006; 26:6911–6923. [PubMed: 16807321]

Richard SB, Lillo AM, Tetzlaff CN, Bowman ME, Noel JP, Cane DE. Kinetic analysis of Escherichia coli 2-C-methyl-D-erythritol-4-phosphate cytidyltransferase, wild type and mutants, reveals roles of active site amino acids. Biochemistry. 2004; 43:12189–12197. [PubMed: 15379557]

Roscioli T, Kamsteeg EJ, Buysse K, Maystadt I, van Reeuwijk J, van den Elzen C, van Beusekom E, Riemersma M, Pfundt R, Vissers LE, et al. Mutations in ISPD cause Walker-Warburg syndrome and defective glycosylation of alpha-dystroglycan. Nature Genetics. 2012; 44:581–585. [PubMed: 22522421]

Ruiz de Almodovar C, Fabre PJ, Knevels E, Coulon C, Segura I, Haddick PC, Aerts L, Delattin N, Strasser G, Oh WJ, et al. VEGF mediates commissural axon chemoattraction through its receptor Flk1. Neuron. 2011; 70:966–978. [PubMed: 21658588]

Sato S, Omori Y, Katoh K, Kondo M, Kanagawa M, Miyata K, Funabiki K, Koyasu T, Kajimura N, Miyoshi T, et al. Pikachurin, a dystroglycan ligand, is essential for photoreceptor ribbon synapse formation. Nature Neuroscience. 2008; 11:923–931.

Satz JS, Barresi R, Durbeej M, Willer T, Turner A, Moore SA, Campbell KP. Brain and eye malformations resembling Walker-Warburg syndrome are recapitulated in mice by dystroglycan deletion in the epiblast. The Journal of Neuroscience. 2008; 28:10567–10575. [PubMed: 18923033]

Satz JS, Ostendorf AP, Hou S, Turner A, Kusano H, Lee JC, Turk R, Nguyen H, Ross-Barta SE, Westra S, et al. Distinct functions of glial and neuronal dystroglycan in the developing and adult mouse brain. The Journal of Neuroscience. 2010; 30:14560–14572. [PubMed: 20980614]

Serafini T, Colamarino SA, Leonardo ED, Wang H, Beddington R, Skarnes WC, Tessier-Lavigne M. Netrin-1 is required for commissural axon guidance in the developing vertebrate nervous system. Cell. 1996; 87:1001–1014. [PubMed: 8978605]

Stalnaker SH, Aoki K, Lim JM, Porterfield M, Liu M, Satz JS, Buskirk S, Xiong Y, Zhang P, Campbell KP, et al. Glycomic analyses of mouse models of congenital muscular dystrophy. The Journal of Biological Chemistry. 2011; 286:21180–21190. [PubMed: 21460210]

Steigemann P, Molitor A, Fellert S, Jackle H, Vorbruggen G. Heparan sulfate proteoglycan syndecan promotes axonal and myotube guidance by slit/robo signaling. Current Biology. 2004; 14:225–230. [PubMed: 14761655]

Sugita S, Saito F, Tang J, Satz J, Campbell K, Sudhof TC. A stoichiometric complex of neurexins and dystroglycan in brain. The Journal of Cell Biology. 2001; 154:435–445. [PubMed: 11470830]

Tachikawa M, Kanagawa M, Yu CC, Kobayashi K, Toda T. Mislocalization of Fukutin Protein by Disease-causing Missense Mutations Can Be Rescued with Treatments Directed at Folding Amelioration. The Journal of Biological Chemistry. 2012; 287:8398–8406. [PubMed: 22275357]

Talts JF, Andac Z, Gohring W, Brancaccio A, Timpl R. Binding of the G domains of laminin alpha1 and alpha2 chains and perlecan to heparin, sulfatides, alpha-dystroglycan and several extracellular matrix proteins. The EMBO journal. 1999; 18:863–870. [PubMed: 10022829]

Vitriol EA, Zheng JQ. Growth cone travel in space and time: the cellular ensemble of cytoskeleton, adhesion, and membrane. Neuron. 2012; 73:1068–1081. [PubMed: 22445336]

Willer T, Lee H, Lommel M, Yoshida-Moriguchi T, de Bernabe DB, Venzke D, Cirak S, Schachter H, Vajsar J, Voit T, et al. ISPD loss-of-function mutations disrupt dystroglycan O-mannosylation and cause Walker-Warburg syndrome. Nature Genetics. 2012; 44:575–580. [PubMed: 22522420]

Williamson RA, Henry MD, Daniels KJ, Hrstka RF, Lee JC, Sunada Y, Ibraghimov-Beskrovnaya O, Campbell KP. Dystroglycan is essential for early embryonic development: disruption of Reichert's membrane in Dag1-null mice. Human Molecular Genetics. 1997; 6:831–841. [PubMed: 9175728]

Xiao T, Staub W, Robles E, Gosse NJ, Cole GJ, Baier H. Assembly of lamina-specific neuronal connections by slit bound to type IV collagen. Cell. 2011; 146:164–176. [PubMed: 21729787]

Yan D, Lin X. Shaping morphogen gradients by proteoglycans. Cold Spring Harbor Perspectives in Biology. 2009; 1:a002493. [PubMed: 20066107]

Yuan W, Zhou L, Chen JH, Wu JY, Rao Y, Ornitz DM. The mouse SLIT family: secreted ligands for ROBO expressed in patterns that suggest a role in morphogenesis and axon guidance. Developmental Biology. 1999; 212:290–306. [PubMed: 10433822]

Zou Y, Stoeckli E, Chen H, Tessier-Lavigne M. Squeezing axons out of the gray matter: a role for slit and semaphorin proteins from midline and ventral spinal cord. Cell. 2000; 102:363–375. [PubMed: 10975526]

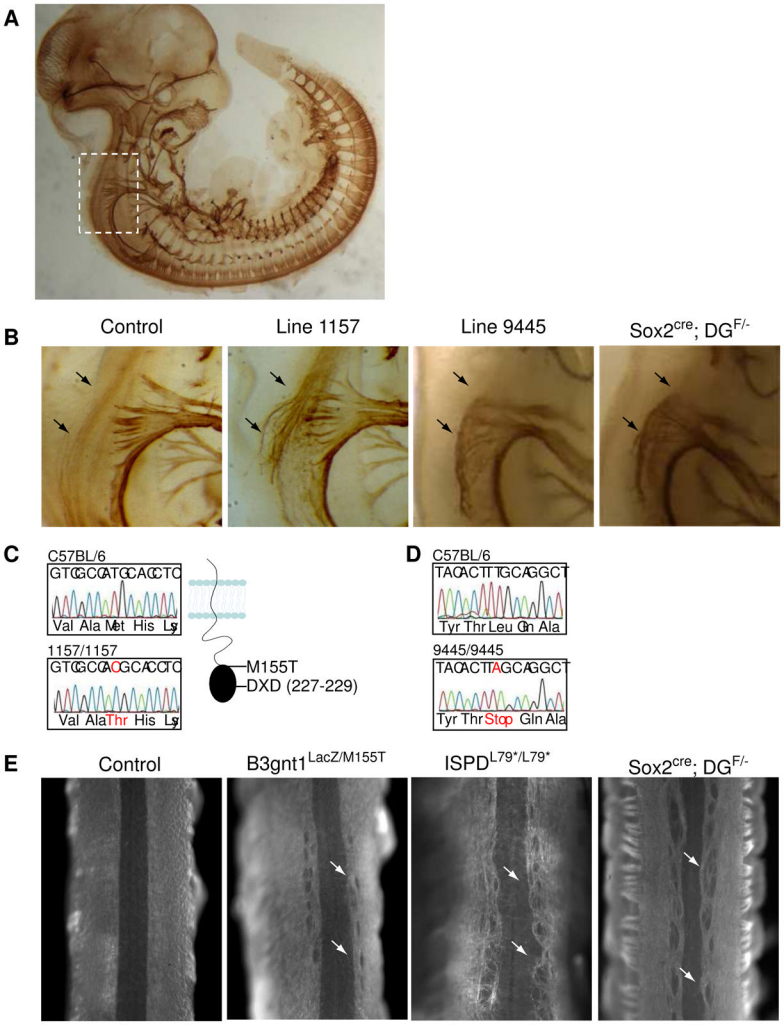

Figure 1. A forward genetic screen identifies *B3gnt1* and *ISPD* as regulators of axon guidance *in vivo*

(A) A sample E11.5 embryo stained using the wholemount neurofilament assay. (B) Lines 1157 and 9445 exhibit axon guidance defects in the hindbrain, highlighted by the boxed area in (A). Control embryos have a tightly fasciculated axon bundle (arrows) that passes dorsally to the vagal nuclei. In contrast, 1157/1157 embryos exhibit defasciculation of this axonal tract, while in 9445/9445 embryos the axon tract is missing, and the central projections of the vagal nerve project aberrantly. Conditional deletion of dystroglycan ($Sox2^{cre}$; $DG^{F/-}$) results in an identical phenotype to line 9445 embryos, with an underdeveloped hindbrain axonal fascicle and misprojections of the vagal central projections. (C) Representative sequencing data from wildtype C57/Ll6 and 1157/1157 embryos showing the T>C mutation in *B3gnt1* that results in conversion of a methionine to threonine at position 155 (M155T). A schematic of B3gnt1 protein structure highlights the location of the M155T mutation in the putative catalytic domain. (D) Representative sequencing data from wildtype C57/BL6 and 9445/9445 embryos showing the T>A mutation in *ISPD* that results in conversion of a leucine to a stop codon (L79*), resulting in an early truncation. (E) Axons from dorsal root ganglia sensory neurons normally bifurcate and project along the anterior-posterior axis of the dorsal spinal cord as a tightly fasciculated bundle, as seen in control embryos at E13. In contrast, the dorsal funciculus in

B3gnt1$^{Lacz/M155T}$, *ISPD*$^{L79*/L79*}$ and Sox2^{cre}; DG$^{F/-}$ mutants is highly defasciculated, with large patches devoid of axons (white arrows).

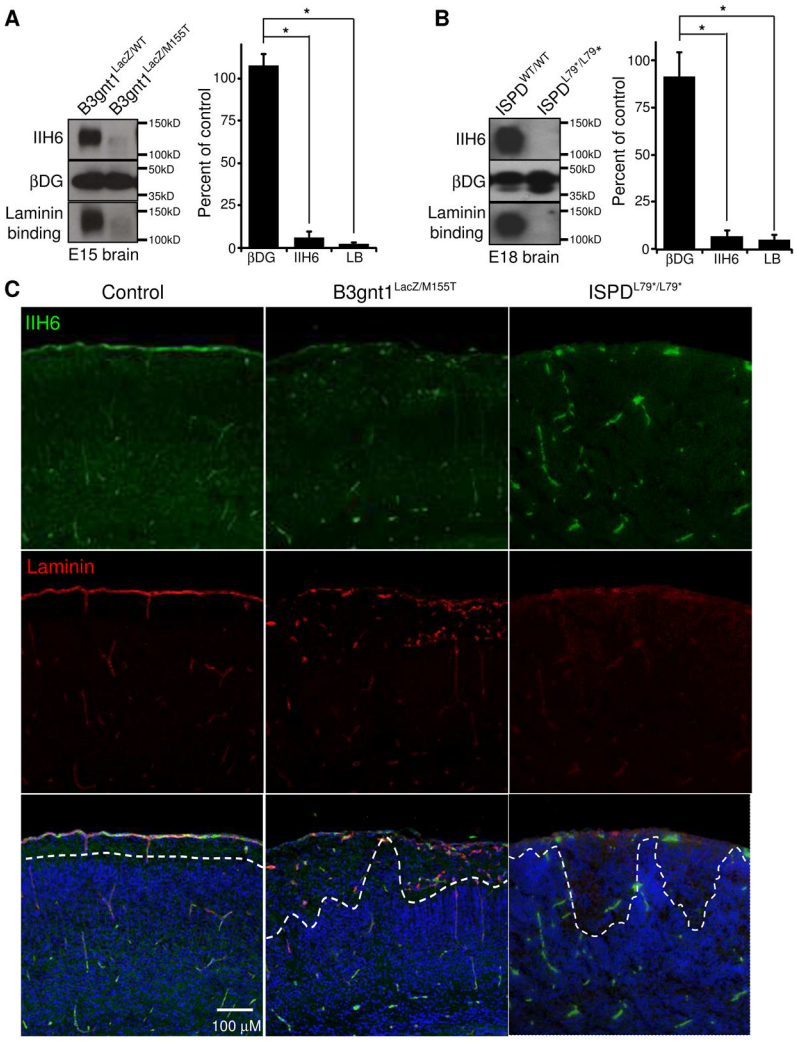

Figure 2. *B3gnt1* and *ISPD* mutants have defective glycosylation of dystroglycan and develop cobblestone lissencephaly

(A–B) WGA-enriched brain lysates show a loss of dystroglycan glycosylation (IIH6) in *B3gnt1*$^{Lacz/M155T}$ and *ISPD*$^{L79*/L79*}$ mutants compared to control embryos, while total dystroglycan levels (β-dystroglycan) remain normal. Lysates from *B3gnt1*$^{LacZ/M155T}$ and *ISPD*$^{L79*/L79*}$ mutants are also defective for laminin binding. Quantification of western blots was done using samples from multiple embryos from separate litters (n=3). (C) Immunostaining of cortical sections shows a loss of glycosylated dystroglycan (IIH6, green) and laminin (red) along the basal surface in *B3gnt1*$^{LacZ/M155T}$ and *ISPD*$^{L79*/L79}$ mutants. Nuclear staining (blue) revealed extensive cortical migration defects characteristic of cobblestone lissencephaly in *B3gnt1*$^{LacZ/M155T}$ and *ISPD*$^{L79*/L79*}$ mutants (dotted lines).

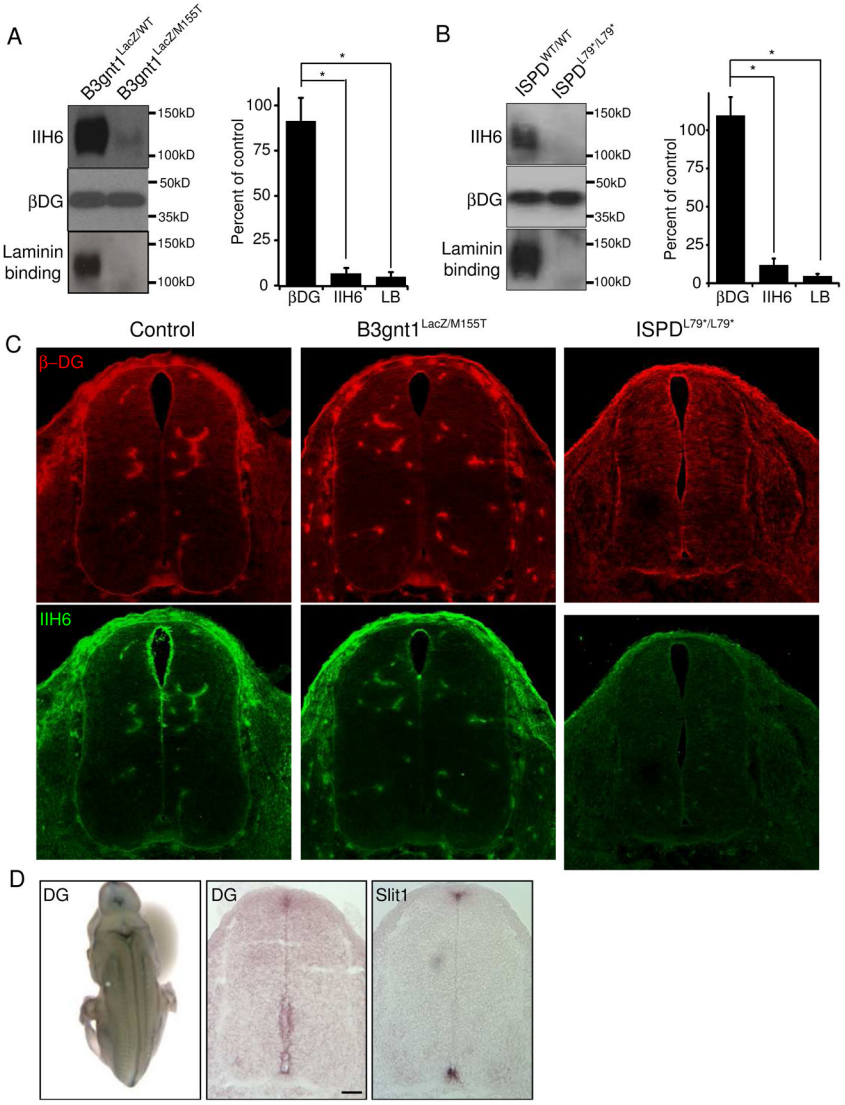

Figure 3. Glycosylation of dystroglycan is defective in the spinal cord of *B3gnt1*$^{LacZ/M155T}$ embryos

(A–B) WGA-enriched spinal cord lysates show deficient dystroglycan glycosylation (IIH6) in *B3gnt1*$^{Lacz/M155T}$ and *ISPD*$^{L79*/L79*}$ mutants compared to control embryos, while total dystroglycan levels (β-dystroglycan) remain normal. Lysates from *B3gnt1*$^{LacZ/M155T}$ and *ISPD*$^{L79*/L79*}$ mutants are also defective for laminin binding. Quantification of western blots was done using samples from multiple embryos from separate litters (n=3). (C) Immunostaining of spinal cords from E11.5 control, *B3gnt1*$^{LacZ/M155T}$ and *ISPD*$^{L79*/L79*}$ embryos showed that β-dystroglycan expression (red, top panels) is enriched in along the basement membrane surrounding the spinal cord, and in the floor plate. In contrast, glycosylated dystroglycan expression (IIH6, green, bottom panels) is deficient in the *B3gnt1*$^{LacZ/M155T}$ and *ISPD*$^{L79*/L79*}$ embryos compared to controls (n=3). (D) *In situ* hybridization shows that *dystroglycan* mRNA (left and middle panels) is expressed in the midline and overlaps with the expression of *Slit1* (right panel) in the floor plate of E12.5 spinal cord (n=3). Scale bar represents 100 μM.

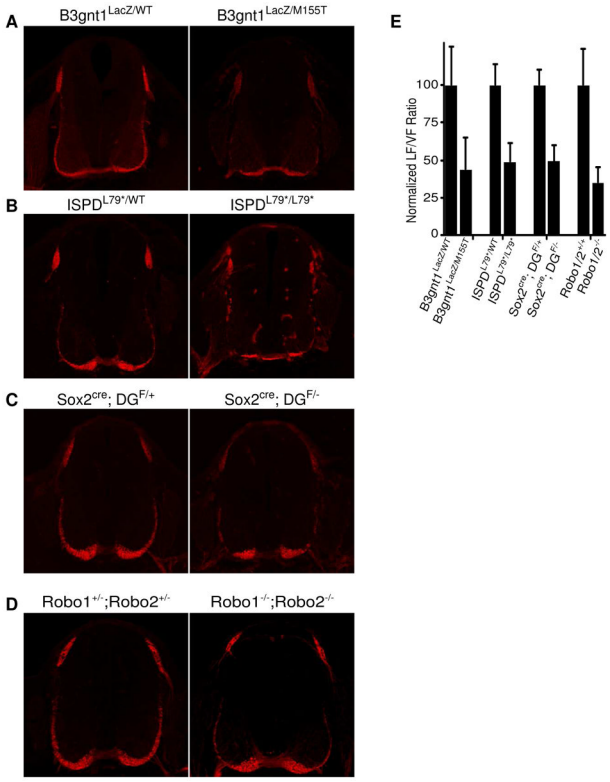

Figure 4. Dystroglycan is required for spinal cord commissural axon crossing and development of the ventrolateral funiculus

(A–C) Spinal cords from E11.5 (A) *B3gnt1*$^{LacZ/WT}$ and *B3gnt1*$^{LacZ/M155T}$ (n=5), (B) *ISPD*$^{L79*/WT}$ and *ISPD*$^{L79*/L79*}$ (n=4), (C) *Sox2*^{cre}*; DG*$^{F/+}$ and *Sox2*^{cre}*; DG*$^{F/-}$ (n=3), and (D) *Robo1*$^{+/-}$; *Robo2*$^{+/-}$ and *Robo1*$^{-/-}$; *Robo2*$^{-/-}$ (n=3) embryos were immunostained for L1 to label post-crossing commissural axons. (E) The area occupied by axons in the ventral funiculus and the lateral funiculus was quantified, expressed as a ratio of LF/VF area and normalized to controls. The motor exit point (white asterisk) was used to demarcate the division between the lateral and ventral funiculi. Scale bar represents 200 μM. Data are represented as mean +/− SD. Statistical analysis was done using a Student's *t* test, * p<0.001.

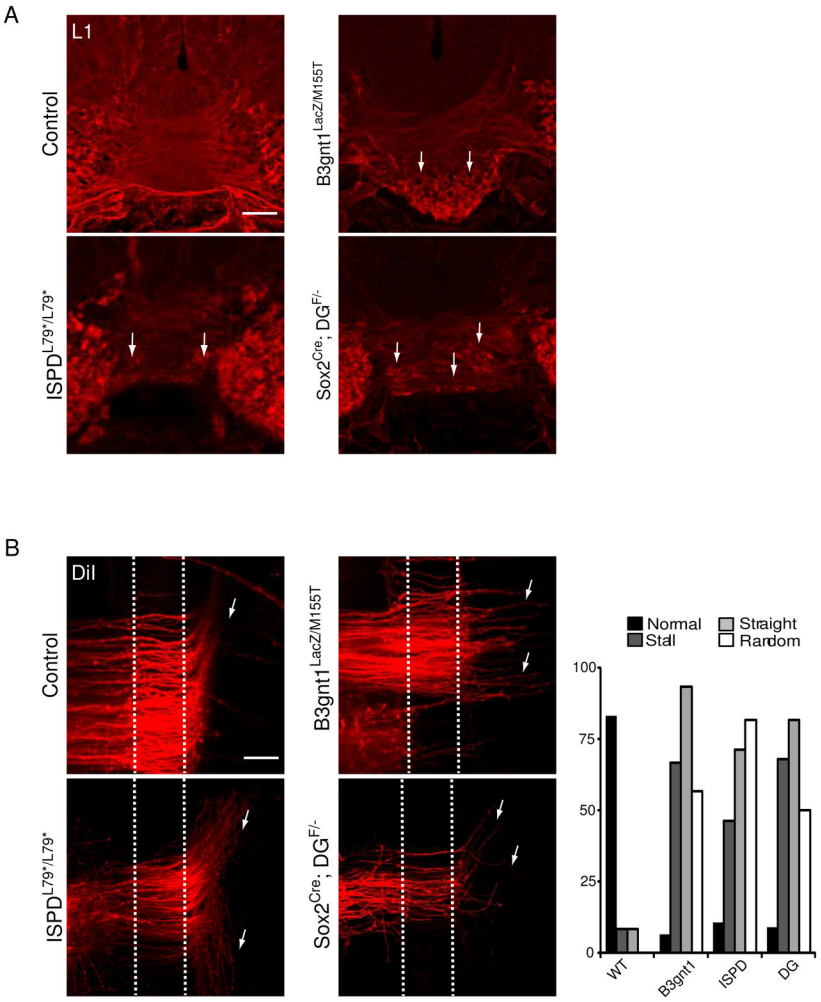

Figure 5. Post-crossing trajectory of commissural axons is disrupted in *B3gnt1* and *dystroglycan* mutants

(A) High magnification images from the floor plate of E13 $B3gnt1^{LacZ/M155T}$ (n=7), $ISPD^{L79*/L79*}$ (n=3), and $Sox2^{Cre}; DG^{F/-}$(n=3) embryos showed L1 positive axons aberrantly projecting within the floor plate (white arrows), in contrast to control embryos (n=5). Scale bar represents 25 μM. (B) DiI injections were performed to unilaterally label commissural axons, and post-crossing axonal trajectory was scored as normal, stalled, straight, or random (indicative of both anterior and posterior turning). Axons from control embryos turned anteriorly (up in images) after crossing the floor plate (dashed white lines), whereas axons from $B3gnt1^{LacZ/M155T}$, $ISPD^{L79*/L79*}$, and $Sox2^{Cre}; DG^{F/-}$ embryos showed abnormal axonal trajectories (white arrows) at all axial levels. Scale bar represents 50 μM. Quantification of axonal trajectory is from three spinal cords per genotype, with at least ten injections per spinal cord.

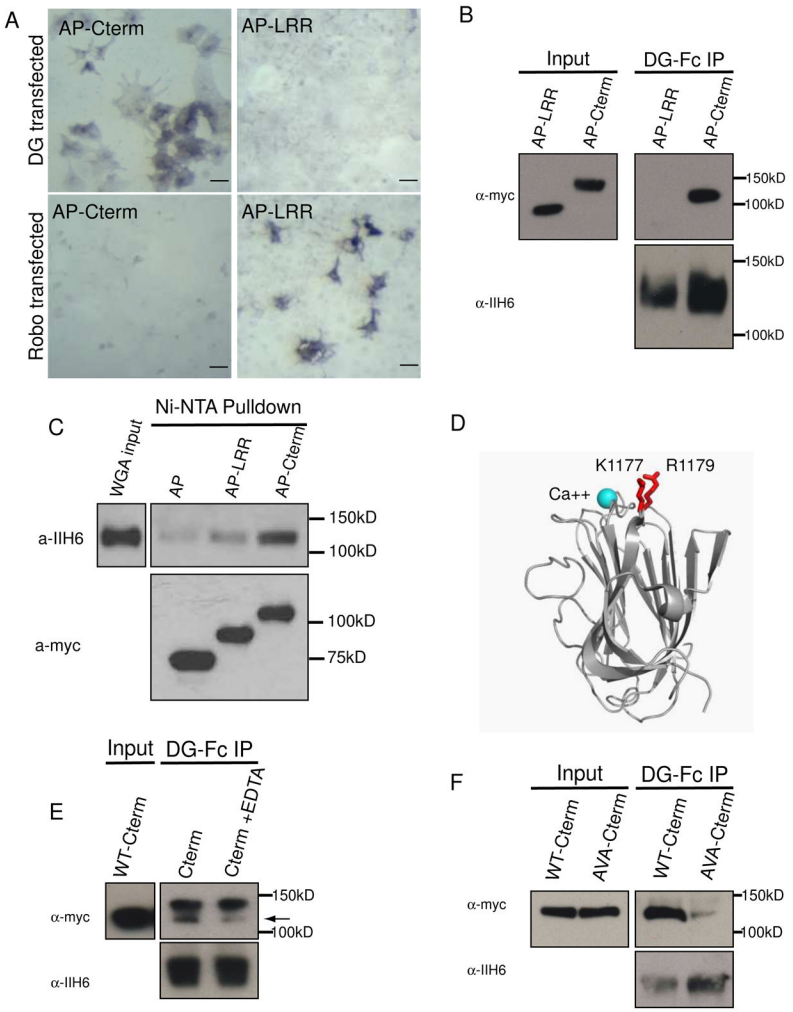

Figure 6. Dystroglycan binds to the C-terminal region of Slit via the Slit laminin G domain

(A) COS7 cells transfected with full-length dystroglycan (top panels) or Robo-1 (bottom panels) were incubated with either AP-Slit2 LRR (containing the Robo binding domain, right panels) or AP-Slit2 C-terminus (containing the Laminin G motif, left panels). Robo transfected cells bound to AP-Slit2 LRR, but not the AP-Slit2 C-terminus, whereas dystroglycan transfected cells bound the AP-Slit2 C-terminus, but not to AP-Slit2 LRR (n=3). Scale bars represent 25 μM. (B) Fc-tagged α-dystroglycan secreted from COS7 cells was incubated with supernatant containing either secreted AP-Slit2 LRR or AP-Slit2 C-terminus, both of which contain a C-terminal myc-tag. DG-Fc was able to associate with AP-Slit2 C-terminus, but not AP-Slit2 LRR (n=3). (C) Secreted AP-Slit2 LRR or AP-Slit2 C-terminus were incubated with WGA-enriched brain lysate, and complexes were purified using Ni-NTA beads. Endogenous brain dystroglycan associates with Slit2 C-terminus, but not Slit2 LRR (n=4). (D) Crystal structure of LG5 from Laminin α1, with a bound Ca^{2+} in blue, and the basic residues corresponding to K1177 and K1179 in the LG domain of Slit2 highlighted in red. (E) DG-Fc association with AP-Slit2 C-terminus requires divalent cations, as addition of EDTA abolished binding (black arrow, n=3). (F) Mutation of basic residues adjacent to the Ca^{2+} binding site (K1177A, K1179A) in the Slit2 C-terminus results in a loss of binding to DG-Fc (n=3).

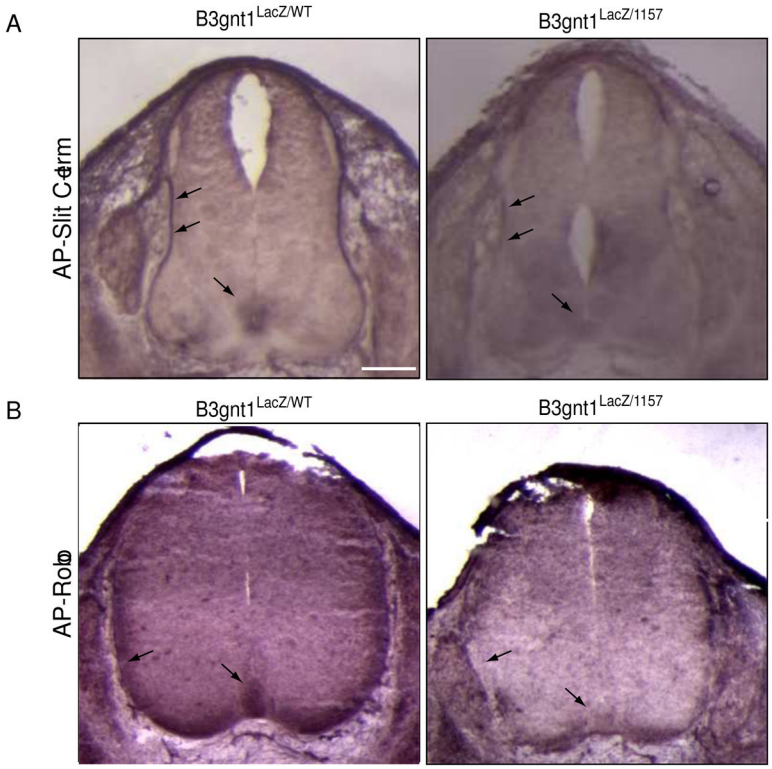

Figure 7. Slit shows aberrant *in vivo* binding and localization in *B3gnt1* mutants

(A) Spinal cord sections from *B3gnt1*$^{LacZ/WT}$ and *B3gnt1*$^{LacZ/M155T}$ embryos were incubated with AP-Slit2 C-terminus to identify endogenous binding sites *in vivo*. The Slit2 C-terminus bound specifically to regions of dystroglycan expression in tissue sections from *B3gnt1*$^{LacZ/WT}$ embryos, including the basement membrane surrounding the spinal cord and the floor plate (arrows, left panel). In contrast, Slit2 C-terminus binding to the basement membrane and floor plate is absent in *B3gnt1*$^{LacZ/1157}$ embryos (arrows, right panel)(n=4). (B) To detect the localization of endogenous Slit protein *in vivo*, spinal cord sections from *B3gnt1*$^{LacZ/WT}$ (left panels) and *B3gnt1*$^{LacZ/M155T}$ (right panels) embryos were incubated with AP-Robo. Binding of AP-Robo is detected in the floor plate and in a gradient along the basal surface of the spinal cord of *B3gnt1*$^{LacZ/WT}$ embryos (arrows, left panel), and this binding is absent in the spinal cord of *B3gnt1*$^{LacZ/M155T}$ embryos (arrows, right panel)(n=3). Scale bar represents 100 μM.